

Pollution assessment of potential ecological hazards of heavy metals in sediment in northern area of the Gulf of Suez as brownfield area, Egypt.

Sara A. Mobarak^{1,2,*}, Hassan I. Farhat¹, Alaa M. Younis³, Sherif Kharbish¹

¹Geology Department, Faculty of Science, Suez University, Suez, 43518, Egypt.

²Egyptian Environmental Affairs Agency, Egypt.

³Aquatic Environment Department, Faculty of Fish Resources, Suez University, Suez, 43518, Egypt.

Abstract:

The present study was carried out to assess sedimentological characters and to evaluate the potential effects of human activities and natural occurrences of heavy metal levels in marine sediments. Ten marine sediment samples from northern area of Suez Gulf were collected and analyzed using different analytical techniques. Metal Pollution Index, Geo-Accumulation Factor, Enrichment Factor, Contamination Factor, Pollution Load Index and Potential Ecological Risk Index were used for ecological assessment. ArcGIS technique was used to interpolate the obtained data in order to create spatial distribution maps. The concentrations of the studied heavy metals descended in the following order $Fe > Al > Co > Cr > Zn > Ti > Ni > V > Hg$. The used indices show that the sediments of Suez Gulf vary from low polluted (northward) to unpolluted (southward). The recorded values of the studied metals in sediments were lower than the levels of the corresponding consensus-based Canadian environmental Quality Guideline. Sand fractions were the main fraction in Suez Gulf sediments. Coarse and medium sand fractions have wide distribution with variable ratios of silt and clays. CM diagram, bivariate diagram and multivariate linear discriminant functions were used for determination of mode of transportation and accumulation mechanism. Results indicated that studied sediments is subjected to high-energy transporting agent and the deposition takes place by rolling and saltation. PCA and dendrogram classify the studied sites into two main categories according to metal concentration, sources, and sediment features. By applying different ecological assessment methods and comparing the obtained data with international guidelines obviously reveals that the metal concentrations in Suez Gulf were in the range of natural unpolluted sediments.

Key Word: Sedimentological characteristics, Heavy metals, Pollution Index, ArcGIS, Suez Gulf.

Date of Submission: 12-10-2021

Date of Acceptance: 27-10-2021

I. Introduction

Rapid increase in urbanization and industrialization are the major reasons for the continuous discharge of large quantities of heavy metals from anthropogenic sources into the marine ecosystem. Heavy metals enter the sediments in marine environment via numerous pathways, including fertilization, irrigation, runoff, rivers, deposition of the atmosphere, and land sources, where metal production occurred from by-products of crude oil refining and metal mining.

The marine environment naturally contains non-toxic concentrations of heavy metals. However, the anthropogenic products could increase their concentrations, leading to some ecological problems [1]–[4]. Some metals, such as Fe, Cr, Cu, Ni, Mn, and Zn are necessary for marine organisms, but they may be toxic if present in high concentrations. On the other hand, some metals are considered mostly toxic to the marine life, even if they exist in a little quantity [5], for example Hg, Pb, Cd, and Ag.

Sediments are regarded as the main store and final receiver for the metals discharged into the ecosystem [6]. Aquatic Sediments are classified as an important indicator of aquatic ecosystem health, they contain more than ninety percent of metals accumulations in the aquatic environment [7]–[10]. Also, sediments are considered as an indirect source of heavy metals which could come back into the water column due to changes in both physical and chemical properties of aquatic environment, e.g. salinity, pH, redox potential, mineral content [11]–[16]. Adsorption/desorption processes are influenced by a variety of factors, including particle adsorption characteristics, particle size distribution, particle shape and its surface features. Sediments at different sites not only have different chemical composition but also show a variety of particle sizes, which lead to different heavy metal distributions. So that sediment grain size distributions directly affect heavy metal distribution in aquatic environment [17]–[20]. The heavy metal accumulation in relation to sediment grain size

can indicate different contaminant transport models. Also, particle size distributions as a transport agent can be used to monitor the accumulation of heavy metals in sediments e.g. anthropogenic impacts on aquatic systems [10], [19], [20]. Therefore, in the last few decades, the environmental issues of sediment and soil contamination by heavy metal pollutants have gained increased attention in both developed and developing countries all over the world [21].

The most polluted part of the Red Sea is Suez Gulf [22]. A huge discharge from industrial facilities and sewage is being received in the northern area of the Gulf, where electric power stations, petrochemicals, and fertilizers are the major industries in this region, while the other areas of Suez Gulf are under severe stress due to a lot of crude oil extraction and production processes, onshore and offshore, which lead to increased concentration of heavy metals [7], [10], [23]–[28].

Different calculation methods based on different algorithms may result in inconsistency of contamination evaluation when they are used to evaluate the quality of soil and/or ecological geochemistry of sediments. Therefore, it is of high importance to select an appropriate method to evaluate sediment quality because pollution index is an important tool for processing, analyzing, and conveying raw environmental data to technicians, experts, decision makers and the concerned [29], [30]. Many assessment methods have been developed for the evaluation of heavy metals risk in sediments. There are some previous works which have applied this method on different aquatic environments [4], [7], [24], [30]–[34].

The present work aims to a comprehensive evaluation of the heavy metals to gain a clear understanding of the potential ecological risks of Zn, Fe, Co, Ni, V, Cr, Al, Ti and Hg in the northern part of Suez Gulf sediments. In addition to understand and clarify the textural features as an indication of sedimentological characteristics of Suez Gulf. Also, study the relation between metal distributions and sediment characteristics to identify their possible sources.

II. Material And Methods

I Study area

The Northern part of the Red Sea is an important economically sea area for fishing, oil production and industrial processes. That area has a great importance and has gained a significant attention by the Egyptian government, which established a large industrial and investment area – the North Gulf of Suez Economic Zone [35]. Suez Gulf is locally divided into two main regions, the northern part of the Suez Gulf, which is known as Suez Bay. The Suez Bay is located between longitude 32° 28' - 32° 34' E and latitude 29° 54' - 29° 75' N. The Bay is considered a shallow extension of the Suez Gulf with its main axis in the NE-SW direction with mean depth of 10 m [36], and connected to Suez Canal through the north eastern side of the bay [37].

II Sampling

Ten surficial sediment samples (10 cm thickness) have been collected during October 2018, using VanVeen Grab Sampler to represent perfect samples which have a direct contact with biological and chemical exchange processes. Sampling was carefully done according to the method reported by IAEA (2004). All sites are well distributed over the studied area to give a clear and precise assessment for the environmental status of the Suez Gulf. The ten selected Sites (1-10) are shown in the location map (Fig. 1).

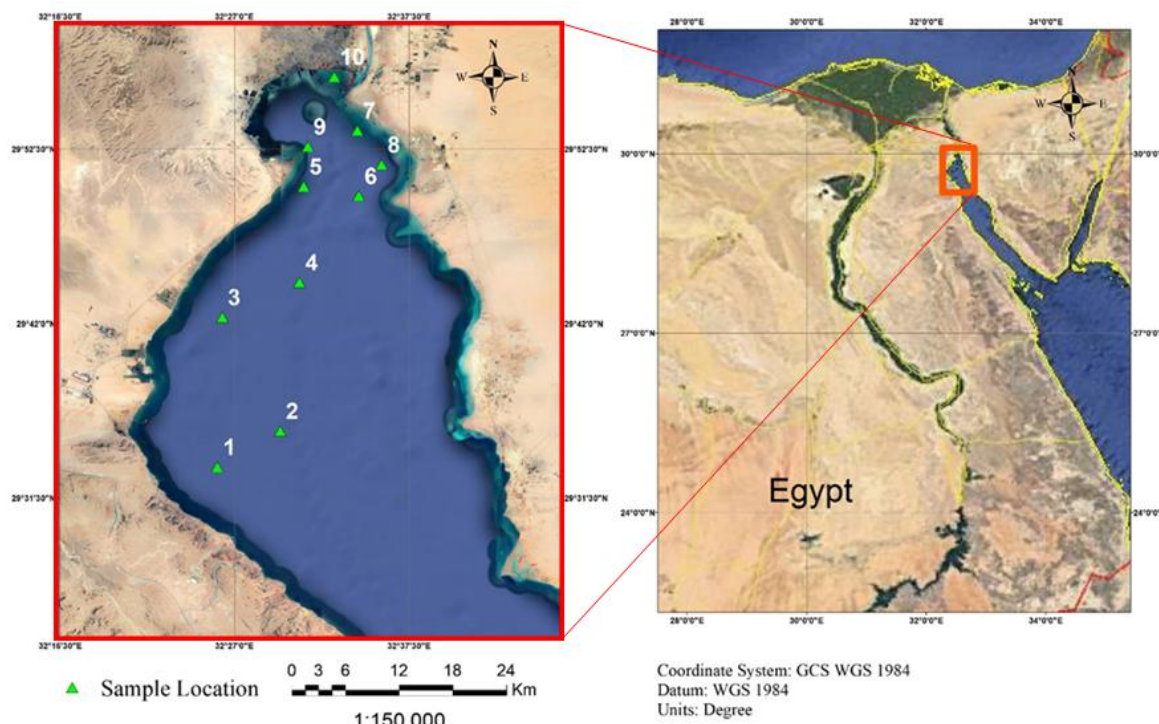


Fig.1 Location map for the studied sediment samples at Suez Gulf.

III Granulometric and chemical Analysis

For grain size analysis, surficial sediment samples were prepared using the decantation method [38], [39], where dry sieving technique was used for grain size analysis [38]. Each sample contains more than 5% mud fraction (finer than 4ϕ) was investigated using the pipette method designated by Carver (1971). According to Folk (1980) textural classes, and sedimentological parameters were calculated.

For mode of transportation and interpretation of depositional environment, the obtained results from grain-size were used in drawing C-M diagram (Where “C” the values of the first percentile are plotted versus “M” the median grain diameter) to identify the mechanics of transportation [41]–[45]. Bivariate diagram were used in to clarify energy of transporting against according to Stewart diagram in which plotting sorting vs median [46].

The deposition environment of Suez Gulf sediments has been explained according to Sahu [47] by using multigroup, multivariant linear discriminant functions. V1 and V2 functions are calculated according to the following equations, adopting the Eigen-vector matrices of Sahu [47]:

$$V_1 = 0.48048M_z + 0.6231(\sigma_I)^2 + 0.40602SK_I + 0.44413K_G \quad (1.a)$$

$$V_2 = 0.24523M_z + 0.45905(\sigma_I)^2 + 0.15715SK_I + 0.83931K_G \quad (1.b)$$

where M_z ; σ_I ; SK_I and K_G are mean size, variance, skewness, and kurtosis, respectively.

For water content (WC.) measurements, WC. was measured using a gravimetric method by oven drying of about 15–20 g wet sediments for 24 h (or to a constant weight) at 105°C . Grinded sediments, sieved to 120 μm , were used to determine organic matter content of the sediments by loss on ignition [48]

For heavy metal determination, using Inductively Coupled Plasma-Mass Spectrometer ICP-MS, a representative 1 gram of sample is digested with repeated additions of nitric acid (HNO_3) and hydrogen peroxide (H_2O_2) and Hydrochloric acid (HCl). 1 g sample was digested with 7.5 mL concentrated HNO_3 , 1.5 mL H_2O_2 and 2.5 mL concentrated HCl in Microwave vessel and complete to the mark of vessel and choose sediment digestion program. Then it was heated using a precisely controlled programmer heating in several ramping and holding cycles until the sample dryness. After the dryness is obtained and after digestion complete let vessel cool before opening. Then sample was carried back into the solution using hydrochloric acid (HCl). With this digestion, certain phases may be soluble partially. The fused sample is diluted and analyzed by Varian 810/820-MS ICP Mass Spectrometers at (Reference Lab. for Drinking Water and Wastewater). Sample treatment and measurement procedures utilizing ICP-MS were published elsewhere [49]–[55].

IV Assessment of ecological risk

For studying the ecological risk and the metal pollution levels caused by the high concentrations of these pollutants in the Northern part of the Suez Gulf, many assessment methods of heavy metals in sediments

were used: Geo-Accumulation Factor (Igeo), Metal Pollution Index (MPI), Contamination Factor (CF), Enrichment Factor (EF), Pollution Load Index (PLI) and Potential Ecological Risk Index (PERI) (Table 1). Different reference values include the Interim Sediment Quality Guideline [57], the Probable Effect Level (PEL) [58], Sediment Quality Guidelines (ERL and ERM) [59], the average shale content [60] and the upper continental crust (UCC) composition were used in this study to represent the pre-industrial reference level of trace/heavy metals [61] (Table 3).

Metal Pollution Index (MPI)

MPI, which was suggested by Usero, was used to assess the total concentration of metals at various sample locations. It is determined according to the formula below [62]:

$$MPI = \sqrt[n]{(C_{s1}^i \times C_{s2}^i \times C_{s3}^i \times \dots \times C_{sn}^i)} \quad (2)$$

where C_{sn}^i is the metal concentration (i) expressed in $\mu\text{g/g}$ of dry weight and n, is the number of metals, while high MPI reveals a high level of pollution with a metal (i) in the sample.

Geo-Accumulation Factor (Igeo)

The geo-accumulation index was calculated by Müller (1969, 1979) and was illustrated by Boszke (2004) according to the following equation:

$$Igeo = \log_2 (C_s^i / 1.5 C_b^i) \quad (3)$$

where C_s is the concentration of a particular metal (i) in the sample, and C_b is the concentration of its background or reference. For the probable variations of the background data due to lithological variations, factor 1.5 is used.

Enrichment Factor (EF)

The Metal Enrichment Factor (EF) is another useful pollution index to distinguish the levels of anthropogenic metal/metalloid pollution. It is defined as follows:

$$EF = \frac{(C_s^i / C_s^{Fe})_{sample}}{(C_b^i / C_b^{Fe})_{crust}} \quad (4)$$

where EF is the enrichment factor, $(C_s^i / C_s^{Fe})_{sample}$ is the concentration of metal divided by Fe concentration in the sample, and $(C_b^i / C_b^{Fe})_{crust}$ is the concentration of the same metal divided by Fe concentration in the earth crust [66]–[70]. EF is the most common and simple method used to evaluate the anthropogenic impact on the sediment.

Contamination Factor (C_f^i)

Contamination factor C_f is one of the most basic approaches of contamination evaluation of metals in the investigated locations. It is calculated by dividing the concentration of metal in the sample by the concentration of the same metal in the reference or background area. C_f equation is expressed by Hakanson (1980) as follows:

$$C_f^i = C_s^i / C_b^i \quad (5)$$

where C_f is the contamination factor, C_s is the metal concentration in the sample, and C_b is its background (reference) concentration.

Pollution Load Index (PLI)

The pollution load index (PLI) was determined using the following equation [72]:

$$PLI = \sqrt[n]{(C_{f1}^i \times C_{f2}^i \times C_{f3}^i \times \dots \times C_{fn}^i)} \quad (6)$$

where PLI is the pollution load index, C_f is the contamination factor; and n is the number of investigated metals.

Potential ecological risk index for single heavy metal pollution (E_r^i)

The following equation clarifies the potential ecological risk index for single heavy metal contamination:

$$Er_r^i = T_r^i \times C_f^i \quad (7)$$

where, T_r^i is the standardized response coefficient for the toxicity of a particular heavy metal. The formula shows the hazardous effect of heavy metals on the human and marine ecosystem and reflects the toxicity level of heavy metals and ecological sensitivity toward the heavy metal contamination. The response coefficient for heavy metal toxicity, which was evolved by Hakanson (1980), was implemented to be an

evaluation standard. Respectively, the corresponding coefficients based on its toxicity were: Hg=40, Ni=Co=5, Cr=V=2, Zn=Fe=Ti=1 [73].

Potential Ecological Risk Index for a variety of heavy metals in sediment (RI)

The equation of potential toxicity response index for several heavy metals was described as follows [71], [74]:

$$RI = \sum_{i=1}^n E_r^i \quad (8)$$

The categories used for the interpretation of all previous indices are given in Table 1.

V Statistical analysis

To determine possible relationships between various variables, the most popular multivariate statistical methods used in ecological studies are applied. In present study, Pearson's correlation analysis, principal component analysis (PCA) calculations and Hierarchical cluster analysis (HCA) were performed for the analyzed samples using IBM SPSS Statistics 26 software to identify the interrelations between the studied variables.

Table 1 Terminologies for pollution classes of single and integrated indices.

Index	Value	Classification	Reference
Igeo	$I_{geo} \leq 0$	Uncontaminated	[63], [91]
	$0 < I_{geo} < 1$	Uncontaminated to moderately contaminated	
	$1 < I_{geo} < 2$	Moderately contaminated	
	$2 < I_{geo} < 3$	Moderately to Heavily contaminated	
	$3 < I_{geo} < 4$	Heavily contaminated	
	$4 < I_{geo} < 5$	Heavily to extremely contaminated	
	$I_{geo} \geq 5$	Extremely contaminated	
Ef	$EF < 2$	Deficiency to minimal enrichment	[68], [69]
	$2 \leq EF < 5$	Moderate enrichment	
	$5 \leq EF < 20$	Significant enrichment	
	$20 \leq EF < 40$	Very high enrichment	
	$EF \geq 40$	Extremally high enrichment	
Cf	$Cf < 1$	Low degree of contamination	[70]
	$1 \leq Cf < 3$	Moderate degree of contamination	
	$3 \leq Cf < 6$	Considerable degree of contamination	
	$Cf \geq 6$	Very high degree of contamination	
Cd	$Cd < 8$	Low degree of contamination	[70]
	$8 \leq Cd < 16$	Moderate degree of contamination	
	$16 \leq Cd < 32$	Considerable degree of contamination	
	$Cd \geq 32$	Very high degree of contamination	
PLI	0	Perfection	[71]
	$0 < PLI < 1$	Baseline levels	
	$PLI > 1$	Progressive deterioration of site	
PERI	$Er < 40$	Low risk	[70], [73]
	$40 \leq Er < 80$	Moderate risk	
	$80 \leq Er < 160$	Considerable risk	
	$160 \leq Er < 320$	High risk	
	$Er \geq 320$	Significantly high risk	
	$RI < 150$	Low ecological pollution risk	
	$150 \leq RI < 300$	Moderate ecological pollution risk	
	$300 \leq RI < 600$	High ecological pollution risk	
$RI \geq 600$	Significantly high ecological pollution risk		

Igeo = Geo-Accumulation Index; EF = Enrichment Factor; CF = Contamination Factor; CD = Contamination Degree; PLI = Pollution Load Index; PERI = Potential Ecological Risk Index; Er = Monomial Ecological Risk Index.

III. Result

I Grain-size analysis

For grain-size distribution, the sand fraction was dominant in the study area which varied from a maximum value (100%) at a site (7) to a minimum value (92.4%) at a site (10) with an average value 98.2% (Fig. 2a). Silt fraction values vary from a maximum value (5.9%) at site (10) and was absent at a site (7) with an average value 1.46% (Fig. 2b). Clay fraction values vary from a maximum value (1.7%) at site 10 and was absent at sites (2, 3, 4, 7 and 8) with an average value 0.34% (Fig. 2c). The distribution map clarifies that fine fractions increased northward (Fig. 2 a, b, and c).

II Textural parameters

For Textural parameters, mean size, sorting, skewness, and kurtosis of the studied sediment samples were calculated and presented in Table 2. The mean size varied from medium sand (0.49Ø) to coarse sand (1.62Ø). Generally, sorting of studied sites was moderately sorted. Sorting varied between poorly sorted (1.04 Ø) at site (10) and moderately well sorted (0.61 Ø) at site (3) (Fig. 3a). The skewness was near-symmetrical at all sites except site (1) was fine-skewed (0.15) and site (3) was coarse-skewed (-0.29) (Fig. 3b). Kurtosis were varied between platy-kurtic to leptokurtic (0.63 & 1.3, respectively) (Fig. 3c).

Table 2 Sedimentological parameters of marine sediment samples collected from Suez Gulf.

Site	Median		(Mz) Mean size		(σI) Sorting		Skewness (SKI)		Kurtosis (KG)		Discriminant functions	
	Value(Ø)	Value(Ø)	category	Value(Ø)	category	Value	category	Value	category	V1	V2	
1	1.07	1.11	Medium Sand	0.75	Moderately sorted	0.15	Fine-skewed	0.85	Platy-kurtic	1.322	1.267	
2	1.10	1.14	Medium Sand	0.76	Moderately sorted	0.08	Near symmetrical	0.95	Platy-kurtic	1.353	1.348	
3	0.95	0.97	Coarse Sand	0.61	Moderately well sorted	-0.29	Coarse skewed	0.63	Platy-kurtic	0.860	0.892	
4	1.03	1.03	Medium Sand	0.81	Moderately sorted	0.03	Near symmetrical	0.98	Platy-kurtic	1.351	1.381	
5	1.18	1.17	Medium Sand	0.82	Moderately sorted	-0.01	Near symmetrical	1.02	Lepto-kurtic	1.430	1.450	
6	1.15	1.15	Medium Sand	0.84	Moderately sorted	-0.01	Near symmetrical	1.04	Lepto-kurtic	1.450	1.477	
7	0.45	0.49	Coarse Sand	0.66	Moderately well sorted	0.07	Near symmetrical	1.05	Lepto-kurtic	1.002	1.212	
8	0.85	0.88	Coarse Sand	0.72	Moderately sorted	0.03	Near symmetrical	1.05	Lepto-kurtic	1.224	1.340	
9	1.40	1.40	Medium Sand	0.87	Moderately sorted	0.00	Near symmetrical	0.99	Platy-kurtic	1.584	1.522	
10	1.60	1.62	Medium Sand	1.04	Poorly sorted	0.09	Near symmetrical	1.30	Lepto-kurtic	2.066	1.999	

III Mode of transportation and depositional environmental interpretation

Application of C-M Diagram, by using of C-M diagram, results of grain-size distributions of Suez Gulf sediments have been studied with the intention of explaining the mechanism of transportation and deposition. The C-M diagram is used to study both fluvial and coastal deposits, as both contain different lithofacies, which may be divided into depositional sub-environments using the diagram [2], [75], [76]. According to Passega [41], [42], Passega and Byramjee [43] and Mycielska-Dowgiało and Ludwikowska-Kędzia [45] results indicate that mode of transportation of most of Suez Gulf sediment was saltation and rolling (QP) northwestward (sites 4, 5 & 9), northward (site 10), southwestward (sites 1 & 2) and westward (site 6). While the mode of transportation was rolling at sites 3, 7 and 8 (Fig. 4).

Bivariate plot, bivariate diagram of sorting vs median according to Stewart [46] revealed that all the sediment samples is located away from the area of slow deposition from quite water and affected by high energy transporting agent. This result support the C-M diagram results (Fig. 5).

Multigroup multivariant discriminant functions V1–V2 plot, According to Sahu [47], a precise statistical method of multigroup multivariant linear discriminant functions was used for estimating the environment of deposition of Suez Gulf marine sediments. Results obtained by the discriminant functions of V1 and V2 (Table 2) were plotted on the multigroup multivariant discriminant diagram (Fig. 6). Generally, all sites represent beach environments deposition (only site 10; area facing Suez Canal entrance and Suez Governorate fall in the field of the shallow marine environment). This may be due to water circulation, active wave movements, and low depth of water column which records great wind activities effect on sediment, This result support the C-M diagram & bivariate results.

IV Total organic carbon (TOC)

Organic carbon contents values were increasing northward, the recorded values ranged between 0.74% at site (8) and 1.9% at site (10), with an average value 1% (Fig. 2e). It is clear that fine sediments contained higher organic matter than coarser ones. Coarse sediments usually have larger pores, thus faster circulation and movement of interstitial water and oxygen-rich seawater.

V Carbonate content (CO₃)

Figure 2f shows that carbonate content in the studied sediment samples has minimum value at site (10) (southward) and maximum value at site (7) (north-eastward). Most of studied sediment indicate terrigenous materials with average carbonate value ranges between (20–40%), except site 7 which indicating transitional materials with average carbonate value ranges between (40–60%), according to Maxwell classification [77].

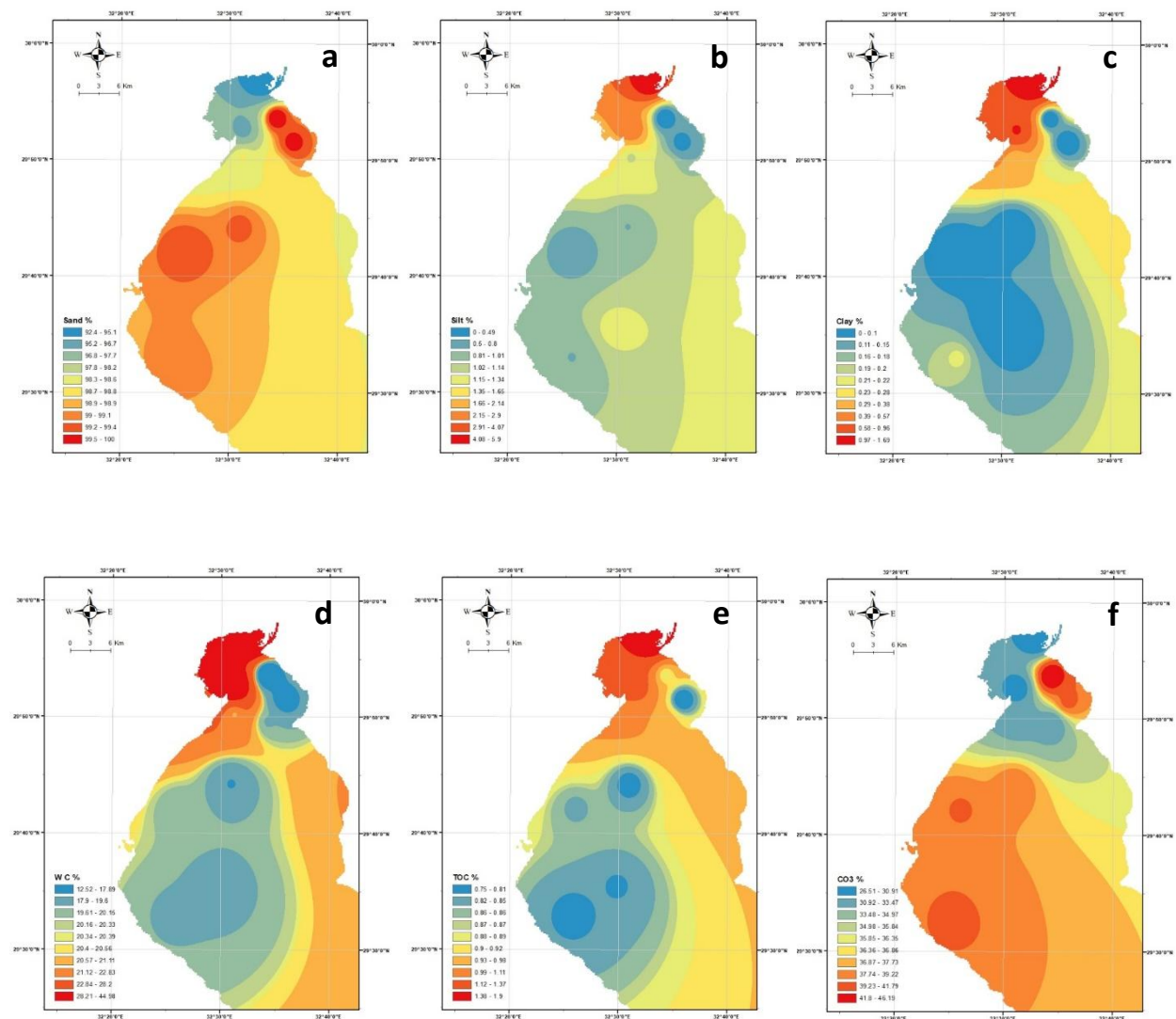


Fig. 2 The spatial distribution of grain sizes in Suez Gulf using GIS techniques (a) sand %, (b) silt %, (c) clay %, (d) Water content %, (e) Total organic carbon % and (f) CO₃%.

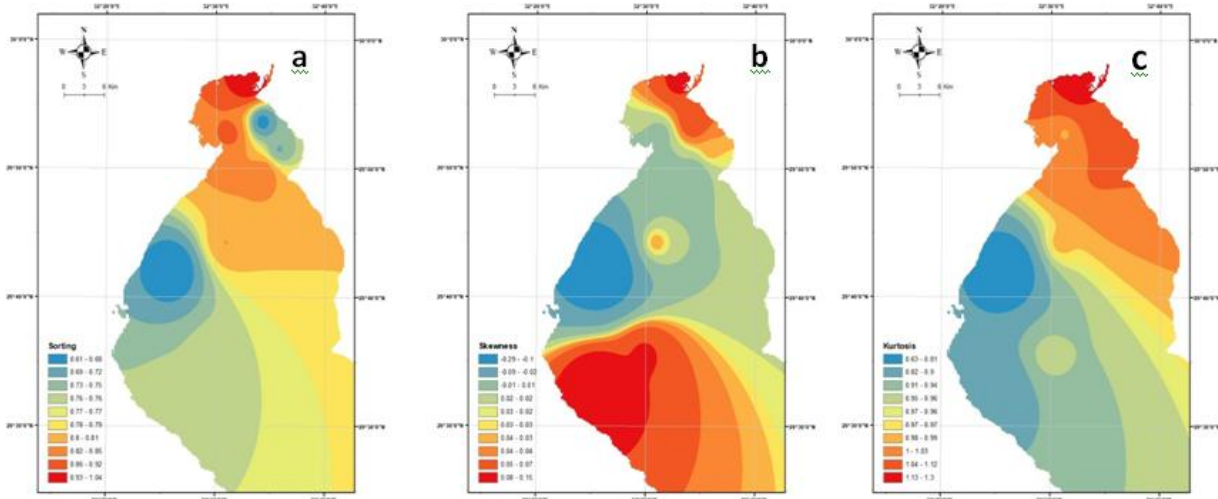


Fig. 3 The spatial distribution of (a) sorting, (b) skewness, and (c) kurtosis for Suez Gulf using GIS techniques.

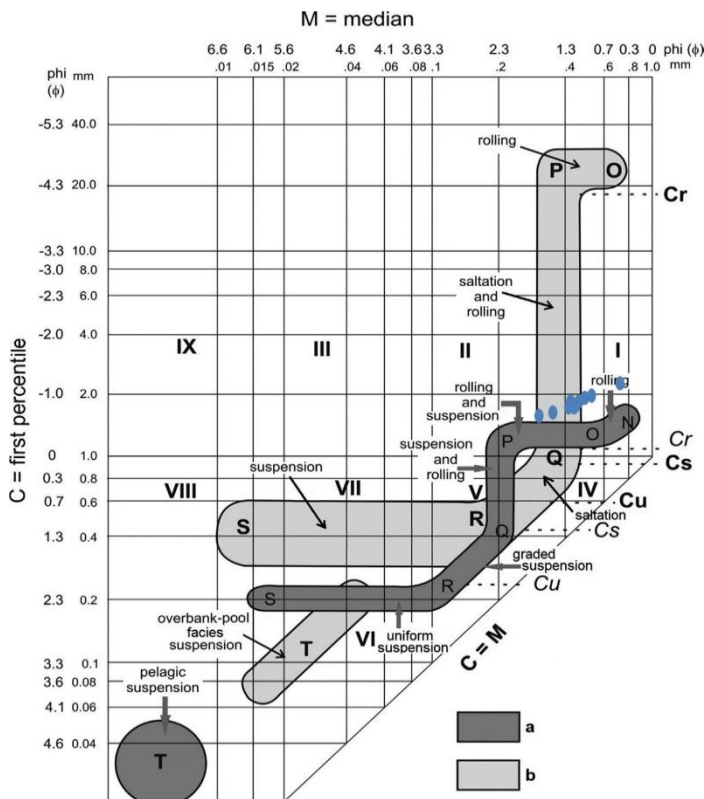


Fig. 4 C-M diagram showing mode of transportation for Suez Gulf (a: according to Passega [42] and Passega & Byramjee [43]; b: according to Ludwikowska-Kędzia [75]).

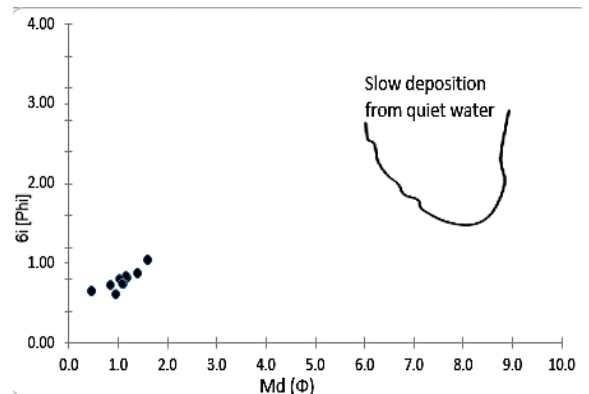


Fig. 5 Bivariate plot of sorting vs. medians showing Energy process diagram for Suez Gulf. [46].

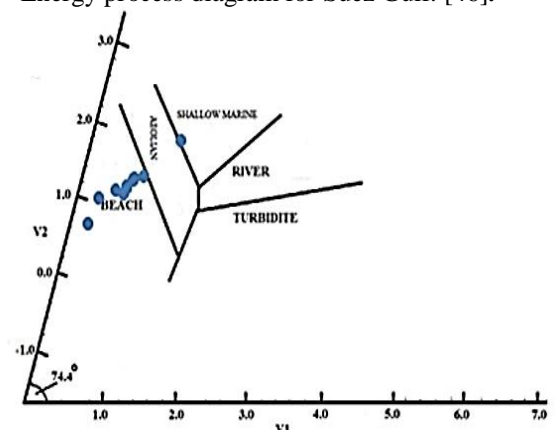


Fig. 6 Multigroup multivariate discriminant functions V1-V2 plot for Suez Gulf.

VI Heavy metal distribution

Figures 7 a, b, c, d, e, f, g, and h illustrate the spatial distribution concentrations of heavy metals Fe, Zn, Co, Ni, V, Cr, Ti, and Al in the studied sediment which were collected from the Northern part of Suez Gulf, respectively. The Hg concentration was under the detection limit (ND) at all sampling sites, while Fe, Co, Cr, Zn, Ti, Ni, and V recorded their highest concentration values at the northern part of the Gulf, except Al showed the highest values at the middle part of the Gulf. The southwest part of the studied area showed low concentration of studied heavy metals except V which showed moderate concentration at that area.

Fe concentrations ranged between 167.59 mg/kg at site (4) to 588.56 mg/kg at site (9). Zn concentration ranged between 9.19 mg/kg at site (3) and 46.34 mg/kg at site (5). Co concentration ranged between 8.02 mg/kg at site (1) to 44.25 mg/kg at site (8). Ni concentration ranged between 1.18 mg/kg at site (2) and 13.79 mg/kg at site (6). V concentration varied from 3.14 mg/kg at site (2) to 14.65 mg/kg at site (9). Cr concentrations ranged between 20.10 mg/kg at site (7) and 23.10 mg/kg at site (8). Al concentrations varied from 101.90 mg/kg at site (2) to 700.60 mg/kg at site (5). Ti ranged from 1.04 at site (3) to 15.89 mg/kg at site (8). The concentrations of the studied heavy metals descended in the following order Fe > Al > Co > Cr > Zn > Ti > Ni > V with average concentrations of 312 > 301.37 > 29.13 > 21.68 > 20.58 > 7.48 > 5.94 mg/kg, respectively.

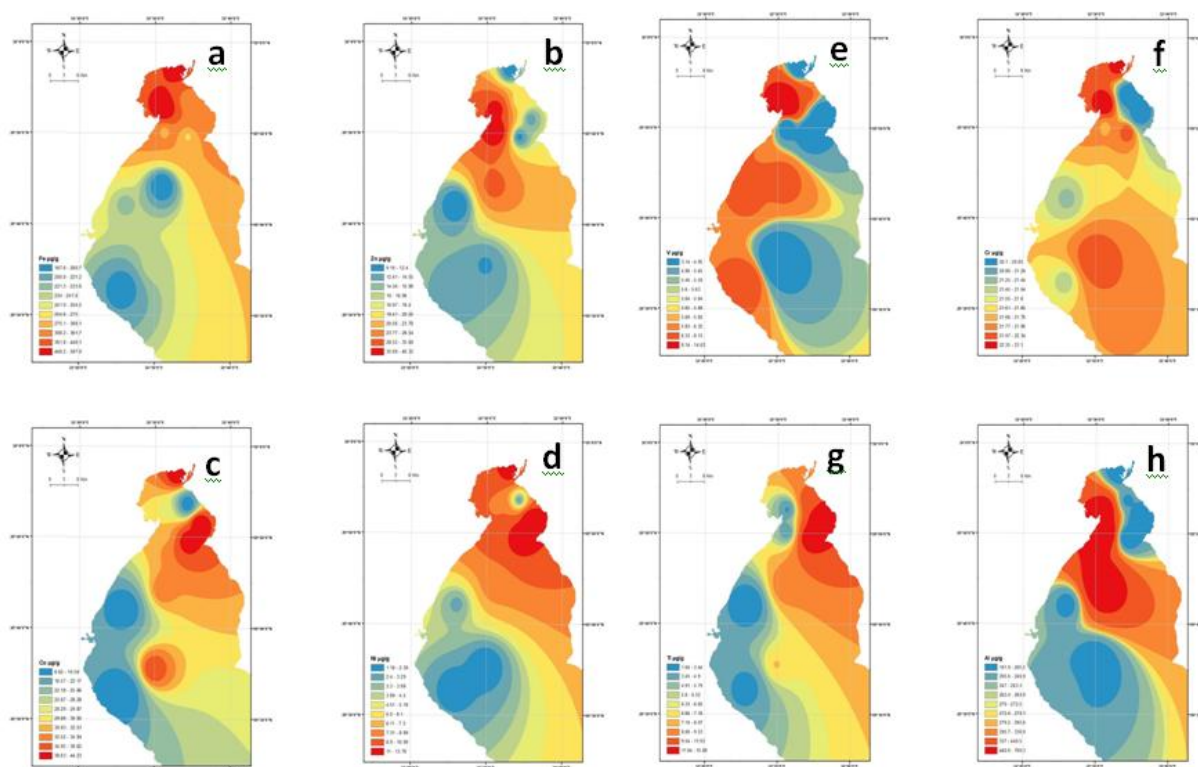


Fig. 7 The spatial distribution of heavy metals in Suez Gulf using GIS techniques (a) Fe, (b) Zn, (c) Co, (d) Ni, (e) V, (f) Cr, (g) Ti, and (h) Al.

Table 3 Comparison of mean concentration of metals recorded in present study with similar published studies, geochemical background, and the toxicological reference values.

Location	Parameters (mg/Kg)									Reference
	Fe	V	Zn	Co	Ni	Cr	Al	Ti	Hg	
Suez Gulf, Egypt	312.36	5.94	20.58	29.13	7.48	21.68	301.37	7.71	ND	Present study
Suez Gulf, Egypt	2384	-	22.4	-	2.89	-	-	-	-	[29]
Suez Gulf, Egypt	4114	-	47.59	-	46.47	26.42	-	-	0.065	[4]
Suez Gulf, Egypt	504.4	-	64.82	12.29	14.91	13.64	-	-	-	[26]
Suez Gulf, Egypt	2511.982	-	85.28	-	14.843	24.113	-	-	-	[24]
Aqaba Gulf, Egypt	544.8	-	35.1	11.2	13.9	7.9	-	-	-	[87]
Aqaba Gulf, Egypt	3150.242	-	58.23	-	13.032	5.775	-	-	-	[24]
Red Sea, Egypt	3072.683	-	75.04	-	28.933	29.899	-	-	-	[24]
Red Sea, Egypt	14562.5	29.78	27.59	4.81	14.33	53.84	-	0.17	-	[32]
Red Sea, Egypt	-	0.49	15.24	-	7.54	-	699.6	-	-	[31]
Red Sea, Egypt	3490	-	22.636	9.696	11.404	18.465	-	-	0.024	[86]
Hurghada area, Egypt	2600	-	12.41	-	7.21	-	-	-	0.02	[79]
Adriatic Sea, Italy	8800	-	95.8	-	-	-	-	-	0.28	[84]
Black Sea, Turkey	5000	-	33.9	-	13.55	-	-	-	-	[85]
Earth's crust	56300	135	70	25	75	100	82300	5700	0.25	[60]
Average shale content	47200	130	95	19	68	90	80000	4600	0.4	[59]
Sediment quality guidelines (ERL)	-	-	150	-	20.9	81	-	-	0.15	[58]
Sediment quality guidelines (ERM)	-	-	410	-	51.6	370	-	-	0.71	
Probable effects level (PEL)	-	-	271	-	42.8	160	-	-	0.7	[56], [57]
Threshold effect level (TEL)	-	-	124	-	15.9	52.3	-	-	0.13	

VII Metal pollution assessment

For the studied sites in the Suez Gulf, all CF values of Fe, Ni, Al, Ti, V, Zn, and Cr indicate low contamination factors (CF), except Co values were ranged between low and moderate CF categories. Contamination degree (Cd) values were in low degree of contamination range (Table 4 & Fig. 8 a). With the same trend of CF, geo-accumulation index (Igeo) indicates uncontaminated sediments for all the analyzed metals in the studied area (Igeo < 0; refers to unpolluted sediments); except for Co where Igeo for Co ranged from uncontaminated to moderately contaminated Igeo values of sites (8), (10), (6) and (2) were 0.24, 0.21, 0.17 and 0.02, respectively (Table 5).

The average EF values for Co, Zn, and Cr were all higher than 40, these elements were considered as extremely high enriched. While the average EF values of Ni and V were less than 20 and were considered as significantly enriched. In all samples, the average EF value for Al and Ti were determined to be less than 2 and were considered as deficient to minimally enriched (Table 6).

MPI results show that the highest metal pollution indices were recorded at sites (9), (4), and (5) (37.35, 32.82, and 31.22, respectively) followed by sites (8), (10), (6) and (7) (28.55, 26.44, 26.15 and 21.81 respectively); while site (3) recorded the lowest MPI (14.01). The high MPI may be caused by marine transportation, industrial activity, and the high human activities in these areas (Table 4 & Fig. 8 b).

For evaluating the potential risk caused by heavy metals Fe, Zn, Co, Ni, V, Cr, and Ti to the aquatic ecosystem in the Suez Gulf surface sediments, among the analyzed heavy metals, Co reported the greatest ecological risk, due to its high toxicity factor. The mean value of E_r^i of Co is 5.826 ± 2.929 , which indicates that Co concentrations vary across the investigated area. The E_r^i values for Co are lower than 40 indicating low risk from Co at all sites. However, investigated area recorded $E_r^i < 40$ for the other six metals (Ni, Cr, Zn, V, Fe and Ti) where their corresponding averages were 0.499 ± 0.326 , 0.434 ± 0.019 , 0.294 ± 0.192 , 0.088 ± 0.052 , 0.006 ± 0.002 and 0.001 ± 0.001 , respectively (Table 7).

The ecological risk index RI of the studied sites has recorded values ranging from the minimum value 2.45 at site (1) (southward) to the maximum value 10.43 at site (7) (north-eastward). Overall, the recorded values at all sites were less than 150, and this clarifies that the marine ecosystem in the studied sediments of Suez Gulf records low ecological pollution risk (Table 7 & Fig. 8 c).

The recorded values of the studied metals in sediments were beneath the levels of the corresponding consensus-based TEL, PEL, ERL, ERM and this indicates that adverse effects do not occur regularly for all investigated area (Table 3).

Co was substantially correlated with Ni ($p < 0.05$), indicating that similar geochemical behavior or origin are likely related. While clay, silt, Water Content, and TOC showed a strongly positive correlation ($p < 0.01$) indicating similar sedimentological behavior. Sand had a significant negative correlation with Water Content and TOC while showing a positive correlation with CaCO_3 ($p < 0.01$) that may indicate that the sand fraction contains shell fragments. Though, no statistical correlation was observed among Al, Zn and Co. This result indicates the different input sources of Co from these two elements (Table 8).

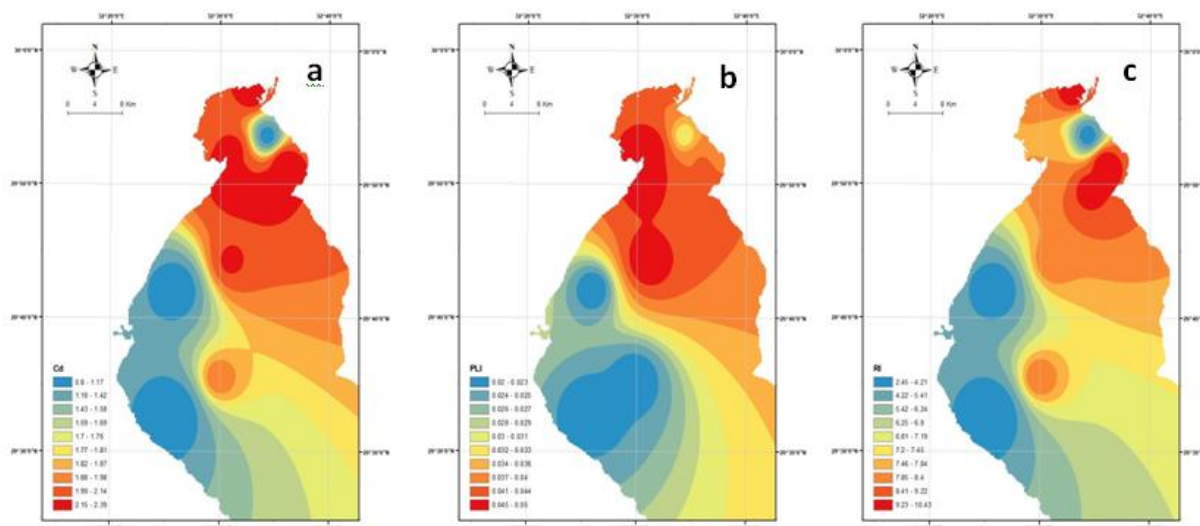


Fig. 8 The spatial distribution of a) Cd, b) PLI, and c) RI in Suez Gulf using GIS techniques.

Table 4 Contamination factors (CF), Contamination degree (Cd), Mean contamination degree (mCd), Pollution load index (PLI) and Metal Pollution Index (MPI) for different heavy metals in Suez Gulf sediments.

Site	CF									mCd	PLI	MPI
	Fe	V	Zn	Co	Ni	Cr	Al	Ti	Cd			
1	0.0033	0.05	0.19	0.32	0.02	0.22	0.0027	0.0005	0.80	0.10	0.02	15.27
2	0.0043	0.02	0.17	1.52	0.02	0.22	0.0012	0.0013	1.96	0.25	0.02	16.90
3	0.0041	0.05	0.13	0.36	0.04	0.21	0.0021	0.0002	0.81	0.10	0.02	14.01
4	0.0030	0.05	0.44	1.37	0.10	0.22	0.0084	0.0016	2.20	0.27	0.05	32.82
5	0.0052	0.03	0.66	1.29	0.13	0.22	0.0085	0.0007	2.34	0.29	0.05	31.22
6	0.0048	0.03	0.16	1.69	0.17	0.22	0.0014	0.0025	2.29	0.29	0.04	26.15
7	0.0057	0.05	0.27	0.40	0.04	0.20	0.0023	0.0019	0.97	0.12	0.03	21.81
8	0.0060	0.03	0.19	1.77	0.18	0.20	0.0016	0.0028	2.39	0.30	0.04	28.55
9	0.0105	0.11	0.57	1.18	0.12	0.23	0.0069	0.0006	2.23	0.28	0.05	37.35
10	0.0087	0.03	0.15	1.74	0.17	0.23	0.0015	0.0015	2.32	0.29	0.04	26.44
Min.	0.0030	0.02	0.13	0.32	0.02	0.20	0.0012	0.0002	0.80	0.10	0.02	14.01
Max.	0.0105	0.11	0.66	1.77	0.18	0.23	0.0085	0.0028	2.39	0.30	0.05	37.35
Av.	0.0055	0.04	0.29	1.17	0.10	0.22	0.0037	0.0014	1.83	0.23	0.04	25.05
SD	0.002	0.026	0.192	0.586	0.065	0.009	0.0030	0.0009	0.68	0.09	0.01	7.89

Table 5 Geo-accumulation Index (*I_{geo}*) of heavy metals in Suez Gulf surface sediments.

Site	Fe	V	Zn	Co	Ni	Cr	Al	Ti
1	-8.84	-4.81	-3.01	-2.23	-6.03	-2.80	-9.13	-11.68
2	-8.46	-6.01	-3.13	0.02	-6.57	-2.75	-10.24	-10.21
3	-8.51	-4.95	-3.51	-2.04	-5.20	-2.81	-9.49	-13.00
4	-8.98	-4.85	-1.76	-0.13	-3.84	-2.80	-7.47	-9.86
5	-8.16	-5.85	-1.18	-0.22	-3.50	-2.79	-7.46	-11.11
6	-8.29	-5.85	-3.19	0.17	-3.10	-2.76	-10.10	-9.21
7	-8.05	-4.97	-2.48	-1.89	-5.20	-2.90	-9.34	-9.59
8	-7.95	-5.74	-2.95	0.24	-3.03	-2.89	-9.92	-9.07
9	-7.16	-3.79	-1.41	-0.34	-3.69	-2.70	-7.77	-11.35
10	-7.43	-5.84	-3.29	0.21	-3.18	-2.73	-9.94	-9.99
Min.	-8.98	-6.01	-3.51	-2.23	-6.57	-2.90	-10.24	-13.00
Max.	-7.16	-3.79	-1.18	0.24	-3.03	-2.70	-7.46	-9.07
Av.	-8.18	-5.27	-2.59	-0.62	-4.33	-2.79	-9.09	-10.51
SD	0.57	0.71	0.84	1.01	1.30	0.06	1.11	1.25

Table 6 Enrichment Factor of heavy metals in marine sediments of Suez Gulf.

Site	V	Zn	Co	Ni	Cr	Al	Ti
1	16.40	56.98	98.33	7.02	65.90	0.82	0.14
2	5.47	40.30	358.69	3.71	52.46	0.29	0.30
3	11.86	32.01	88.85	9.93	52.18	0.51	0.04
4	17.45	148.36	459.70	35.15	72.56	2.84	0.54
5	4.97	126.37	245.33	25.29	41.42	1.62	0.13
6	5.41	34.30	352.16	36.37	46.18	0.28	0.53
7	8.45	47.68	71.47	7.20	35.52	0.41	0.34
8	4.63	32.12	292.57	30.39	33.56	0.26	0.46
9	10.38	54.17	113.33	11.15	22.10	0.66	0.05
10	3.01	17.61	199.98	19.06	26.03	0.18	0.17
Min.	3.01	17.61	71.47	3.71	22.10	0.18	0.04
Max.	17.45	148.36	459.70	36.37	72.56	2.84	0.54
Av.	8.80	58.99	228.04	18.53	44.79	0.79	0.27

Site	Er							RI
	Fe	V	Zn	Co	Ni	Cr	Ti	
1	0.003	0.11	0.19	1.60	0.11	0.43	0.0005	2.45
2	0.004	0.05	0.17	7.62	0.08	0.45	0.0013	8.37
3	0.004	0.10	0.13	1.82	0.20	0.43	0.0002	2.69
4	0.003	0.10	0.44	6.84	0.52	0.43	0.0016	8.35
5	0.005	0.05	0.66	6.43	0.66	0.43	0.0007	8.24
6	0.005	0.05	0.16	8.46	0.87	0.44	0.0025	10.01
7	0.006	0.10	0.27	2.02	0.20	0.40	0.0019	3.00
8	0.006	0.06	0.19	8.85	0.92	0.41	0.0028	10.43
9	0.010	0.22	0.57	5.92	0.58	0.46	0.0006	7.76
10	0.009	0.05	0.15	8.68	0.83	0.45	0.0015	10.18

Table 7 Potential risk index of heavy metals in marine sediments of Suez Gulf.

Table 8 Correlation coefficient among metals, total carbonate, Water Content, total organic carbon, and sediment fractions in marine sediments.

	Al	Cr	Co	V	Zn	Ti	Ni	CaCO3	WC	TOC	Sand	Silt	Clay
Al	1												
Cr	0.206	1											
Co	0.009	0.357	1										
V	0.428	0.296	-0.372	1									
Zn	.933**	0.214	0.066	0.431	1								
Ti	-0.347	-0.384	0.581	-0.446	-0.293	1							
Ni	0.111	0.143	.756*	-0.186	0.174	0.561	1						
CaCO3	-0.213	-.834**	-0.574	-0.079	-0.295	0.135	-0.595	1					
WC	0.081	.746*	0.324	0.311	0.130	-0.269	0.364	-.821**	1				
TOC	-0.028	0.577	0.329	0.094	0.043	-0.103	0.410	-.750*	.936**	1			
Sand	0.028	-.670*	-0.392	-0.095	-0.011	0.136	-0.389	.785**	-.965**	-.979**	1		
Silt	-0.046	.677*	0.412	0.057	-0.017	-0.128	0.378	-.780**	.955**	.971**	-.998**	1	
Clay	0.026	.633*	0.322	0.206	0.097	-0.157	0.413	-.783**	.972**	.981**	-.983**	.970**	1

** Correlation is significant at the 0.01 level.

* Correlation is significant at the 0.05 level.

** Correlation is significant at the 0.01 level.

* Correlation is significant at the 0.05 level.

Applying hierarchical cluster analysis using Ward's method produced a dendrogram with two main clusters, as presented in Figure 9. The dendrogram includes the concentration of the studied metals Fe, Zn, Co, Ni, V, Cr, Al, and Ti, which separates the samples of studied locations into two main clusters according to the increasing in concentrations. As can be seen in Figure 9, within the range of 10-15, the five heavy metal elements can be roughly divided into two categories: Ni, Ti, V, Zn, Cr, and Co fall into the first category; Fe and Al fall into the second category. Meanwhile, in the first category, Ni, Ti, V, Zn, Cr, and Co were more closely related. When the distance was less than 1, Fe and Al were grouped together, reflecting that the differences between Fe and Al in sediment were small, and pollution by them may be homologous. The results of the cluster analysis agreed with those of principal component analysis, providing a basis for more future investigation and examination of the sources of heavy metal pollution.

Principal Component Analysis PCA, PCA analysis method was used for identifying the possible source of heavy metals in the sediments; the number of variables was divided into two principal components (PCs) as shown in Figure 10. PC1 has highly positive loadings for Water Content, Clay, Mud, Silt, TOC, Fe, Cr, Ni, and Co with that values of 0.979, 0.973, 0.970, 0.962, 0.950, 0.791, 0.747, 0.495, and 0.469, respectively,

while Carbonate and Sand showed highly negative values (-0.970 and -0.886, respectively); PC2 has positive loadings for V, Al, Zn with the corresponding values (0.759, 0.690, 0.657, respectively), while Ti showed highly negative value (-0.809). The PCA component plot also shows the concentration of heavy metals in two zones (Fig. 10), which is highly consistent with the distribution of metals throughout the study area in the two groups.

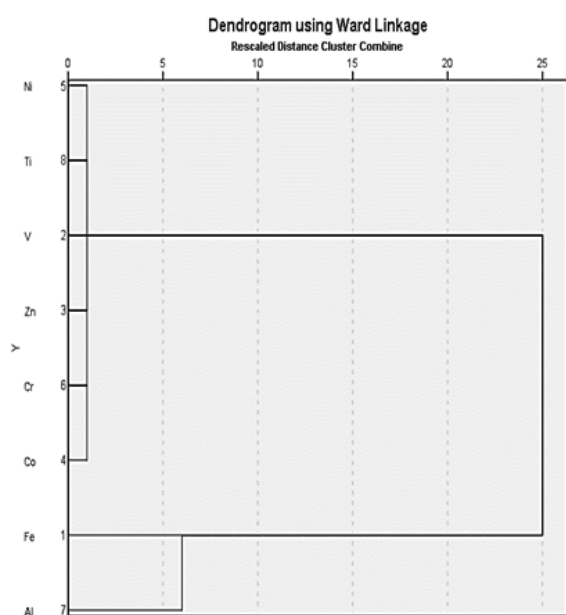


Fig. 9 Dendrogram of cluster analysis showing clusters of metals using ward's method.

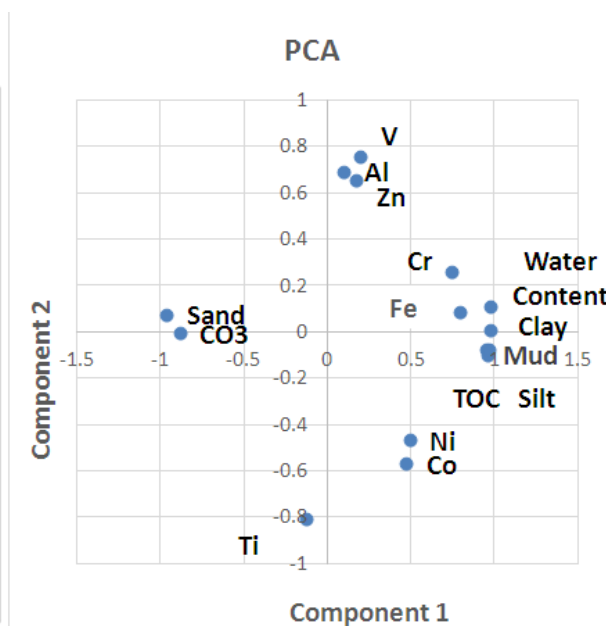


Fig. 10 Principal component analysis (PCA) plot for heavy metals and grain size fractions.

IV. Discussion

Sediments and related ecological studies have gained a great attention lately. The more intensively the land is used, the higher is the risk of erosion and sedimentation problems. Erosion and sedimentation can cause an adverse effect on marine habitat and the species that depend on it. Recognizing, emphasizing and mitigating erosion and sedimentation issues will become crucial for land-use managers and natural resource planners [28], [30], [83].

The textural and depositional characteristics of the studied environment are described by grain size. The particle size distribution in sediment samples is an evidence of the mechanism by which the particles were deposited as well as the presence of various particle sizes in the parent material [80], [84], [85]. Sediment type varies depending on sampling sites. Generally coarse sand was dominant north eastward and southwest areas of the studied location, whereas the rest areas are medium sand. In addition, depth controls the sediment type. It directly proportions with both of mud and clay distribution.

Gulf of Suez sediments were mainly terrigenous origins and composed mainly of sand fraction which varied from medium sand to coarse sand. While the distribution of fine fractions in the studied area was limited, it may be due to low sediment supply, or due to re-transportation of these fractions to deeper areas as results of current action, or both. Results revealed that the increased silt and clay north ward near residential area and torrential outlet. These results are agreed with many previous studies [20], [30], [32], [33]. Mean grain size is mainly controlled by sediments sources. While wide ranges of sorting indicate turbulent conditions [16], [85], [86]. Studied sediment sorting is mainly moderately sorted to moderately well-sorted indicating turbulent conditions. Area is subjected to wave actions and water current which indicate the high-energy transporting environments. Skewness results are mainly near symmetrical indicate that studied area is classified as environments undergoing depositional trends spatially southward. While the negative skewed values of studied sediments indicate high energy environment [87]. The studied sites sediments were platy- to leptokurtic in its nature, these state that the sediment is a combination between a one main population of sand with an insignificant populations of other grain sizes [88]. While bivariate plot supports these results representing that the study area is away from slow deposition from quite area. In addition to the CM and bivariate diagrams reveals that the deposition takes place by rolling and saltation.

The distribution map clarifies that organic carbon increased northward and this is related to the grain size distribution. In general, carbonate content is substantially low in the current studied samples, reflecting the inflow of terrigenous materials. These results are agreed with many previous studies [20], [30], [32]. The results indicate that the measured heavy metals values decrease southwards. By comparing the levels of metals obtained from the present studied sediment samples with local and regional metal levels found in the sediments of similar published work [20], [25], [82], [27], [30], [32], [33], [78]–[81].

The average iron concentration in the present study was beneath those of the other neighboring and worldwide coasts and reference values, while it was along the same line with Youssef and El-Said (2010) regarding the same area. Also, zinc average was beneath those of the other neighboring and worldwide coasts and reference values, but it was in line with Nour and El-Sorogy (2020), while the finding of Nickle was higher. Chromium concentration was higher than those of the other neighboring and beneath worldwide coasts, reference values, Youssef and El-Said (2010), and it was in line with El Zokm et al. (2012) and Ibrahim et al. (2019) for the same area. It is obvious that the present results are in line with most of the previous research and varied from others due to the application of various analytical methods and techniques and sampling sites.

Generally, CF and Cd values in the studied area in Suez Gulf indicate low contamination for most of studied metal, only Co was in moderate category. With the same trend of CF, Igeo and MPI indicates uncontaminated sediments for all the analyzed metals in the studied area ($I_{geo} < 0$; refers to unpolluted sediments); except for Co was moderately contaminated. The measured concentrations of the studied metals were lower than the levels of the corresponding consensus-based TEL, PEL, ERL, ERM and this indicates that adverse effects do not occur regularly for all investigated area. these results are agreed with many previous studies [20], [30], [32], [33].

Correlation analyses were calculated for clarifying relationships between studied metals to provide evidence on their input sources and transportation processes [20], [89]. The results showed that Zn and Al were strongly correlated with each other, suggesting the possibility of their common origin. Co was substantially correlated with Ni, indicating that both have same behavior or origin. Though, no statistical correlation was observed among Al, Zn and Co. This results indicate the different input sources of Co from these two elements.

Applying hierarchical cluster analysis of Fe and Al were grouped together, reflecting that the differences between Fe and Al in sediment were neglected, and pollution by them may be homologous. The results of the cluster analysis agreed with those of principal component analysis, providing a basis for more future investigation and examination of the sources of heavy metal pollution.

PCA has been used to distinguish natural or anthropogenic sources of elements in some studies [18]–[20], [90], [91]. PCA findings indicate that Fe, Cr, Ni, and Co possibly originate from similar sources that may be anthropogenic sources. These metals may be transported under same physiochemical conditions and show similar behavior during transformation [6]. The results also indicate that V, Al, Zn have similar sources that may be natural sources.

V. Conclusion

The present work reveals that sand fraction is the dominant fraction at Suez Gulf. Textural parameters clarify that the area is subjected to wave actions and water current which indicate the high-energy transporting environments. C-M and bivariate diagrams support that the study area is away from slow deposition from quite area, and deposition takes place by rolling and saltation. Suez Gulf sediments adsorb significant quantity of heavy metals at areas facing drains that were under the influence of discharge of industrial wastewater from refinery factories outlets, industrial wastewater treatment plants, sewage treatment plants, electrical planets discharge and harbors, and thus identifying the source of contamination to be from shipping, industrial, sewage, and domestic waste sources. The results illustrate that Suez Gulf status varied between uncontaminated and moderately contaminated thus showing a low ecological risk. In addition to, the sources and origins of heavy metals in Suez Gulf are mainly anthropogenic due to the rapid development in the area and the high growth in population at studied sites. By comparing the obtained data with international guidelines obviously reveals that the metal concentrations were in the range of natural unpolluted sediments.

References

- [1] T. Ntakirutimana, G. Du, J. Guo, X. Gao, and L. Huang, "Pollution and Potential Ecological Risk Assessment of Heavy Metals in a Lake," *Polish J. Environ. Stud.*, vol. 22, no. 4, 2013.
- [2] M. Hu, X. Zhang, Y. Li, H. Yang, and K. Tanaka, "Flood mitigation performance of low impact development technologies under different storms for retrofitting an urbanized area," *J. Clean. Prod.*, vol. 222, pp. 373–380, 2019.
- [3] P. Luo *et al.*, "Water quality trend assessment in Jakarta: A rapidly growing Asian megacity," *PLoS One*, vol. 14, no. 7, p. e0219009, 2019.
- [4] M. I. A. Ibrahim, L. A. Mohamed, M. G. Mahmoud, K. S. Shaban, M. A. Fahmy, and M. H. Ebeid, "Potential ecological hazards assessment and prediction of sediment heavy metals pollution along the Gulf of Suez, Egypt," *Egypt. J. Aquat. Res.*, vol. 45, no. 4, pp. 329–335, 2019, doi: 10.1016/j.ejar.2019.12.003.
- [5] N. U. Saher and A. S. Siddiqui, "Comparison of heavy metal contamination during the last decade along the coastal sediment of

- Pakistan: Multiple pollution indices approach,” *Mar. Pollut. Bull.*, vol. 105, no. 1, pp. 403–410, 2016.
- [6] K. Banat, F. Howari, A. A.-H.-E. Research, and U. 2005, “Heavy metals in urban soils of central Jordan: should we worry about their environmental risks?,” *Elsevier*, 2005, Accessed: Jan. 27, 2021. [Online]. Available: <https://www.sciencedirect.com/science/article/pii/S001393510400132X>.
- [7] H. I. Farhat, “Impact of Drain Effluent on Surficial Sediments in the Mediterranean Coastal Wetland: Sedimentological Characteristics and Metal Pollution Status at Lake Manzala, Egypt,” *J. Ocean Univ. China (Oceanic Coast. Sea Res.*, vol. 18, no. 4, pp. 834–848, Oct. 2019, doi: 10.1007/s11802-019-3608-0.
- [8] J. B. D. A. Camargo, A. C. F. Cruz, B. G. Campos, G. S. Araújo, T. G. Fonseca, and D. M. S. Abessa, “Use, development and improvements in the protocol of whole-sediment toxicity identification evaluation using benthic copepods,” *Mar. Pollut. Bull.*, vol. 91, no. 2, pp. 511–517, 2015.
- [9] Y. A. El-Amier, G. Bonanomi, S. L. Al-Rowaily, and A. M. Abd-ElGawad, “Ecological Risk Assessment of Heavy Metals along Three Main Drains in Nile Delta and Potential Phytoremediation by Macrophyte Plants,” *Plants*, vol. 9, no. 7, p. 910, Jul. 2020, doi: 10.3390/plants9070910.
- [10] P. Zhang, X. Pan, Q. Wang, G. Ge, and Y. Huang, “Toxic effects of heavy metals on the freshwater benthic organisms in sediments and research on quality guidelines in Poyang Lake, China,” *J. Soils Sediments*, vol. 20, no. 10, pp. 3779–3792, 2020.
- [11] Y. Wang, L. Yang, L. Kong, E. Liu, L. Wang, and J. Zhu, “Spatial distribution, ecological risk assessment and source identification for heavy metals in surface sediments from Dongping Lake, Shandong, East China,” *Catena*, vol. 125, pp. 200–205, 2015.
- [12] I. da C. Souza *et al.*, “Changes in bioaccumulation and translocation patterns between root and leaf of *Avicennia schaueriana* as adaptive response to different levels of metals in mangrove system,” *Mar. Pollut. Bull.*, vol. 94, no. 1–2, pp. 176–184, 2015.
- [13] G. Bartoli, S. Papa, E. Sagnella, A. F.-J. of Environmental, and U. 2012, “Heavy metal content in sediments along the Calore river: relationships with physical–chemical characteristics,” *Elsevier*, 2012, Accessed: Jan. 27, 2021. [Online]. Available: <https://www.sciencedirect.com/science/article/pii/S0301479711000545>.
- [14] K. Nemati, N. K. A. Bakar, M. R. Abas, and E. Sobhanzadeh, “Speciation of heavy metals by modified BCR sequential extraction procedure in different depths of sediments from Sungai Buloh, Selangor, Malaysia,” *J. Hazard. Mater.*, vol. 192, no. 1, pp. 402–410, 2011, doi: 10.1016/j.jhazmat.2011.05.039.
- [15] J. P. Vink, “The origin of speciation: Trace metal kinetics over natural water/sediment interfaces and the consequences for bioaccumulation,” *Environ. Pollut.*, vol. 157, no. 2, pp. 519–527, Feb. 2009, doi: 10.1016/j.envpol.2008.09.037.
- [16] A. M. Younis, G. M. El-Zokm, and M. A. Okbah, “Spatial variation of acid-volatile sulfide and simultaneously extracted metals in Egyptian Mediterranean Sea lagoon sediments,” *Environ. Monit. Assess.*, vol. 186, no. 6, pp. 3567–3579, 2014, doi: 10.1007/s10661-014-3639-3.
- [17] Q.-R. Wang, Y.-S. Cui, X.-M. Liu, Y.-T. Dong, and P. Christie, “Soil contamination and plant uptake of heavy metals at polluted sites in China,” *J. Environ. Sci. Heal. Part A*, vol. 38, no. 5, pp. 823–838, 2003.
- [18] T. Okada, P. Lacombe, and C. Mason, “Estimating the spatial distribution of dredged material disposed of at sea using particle-size distributions and metal concentrations,” *Mar. Pollut. Bull.*, vol. 58, no. 8, pp. 1164–1177, 2009, doi: 10.1016/j.marpolbul.2009.03.023.
- [19] C. Liu, J. Cui, G. Jiang, X. Chen, L. Wang, and C. Fang, “Soil heavy metal pollution assessment near the largest landfill of China,” *Soil Sediment Contam. An Int. J.*, vol. 22, no. 4, pp. 390–403, 2013.
- [20] L. Feng, C. Hu, X. Chen, and X. Zhao, “Dramatic inundation changes of China’s two largest freshwater lakes linked to the Three Gorges Dam,” *Environ. Sci. Technol.*, vol. 47, no. 17, pp. 9628–9634, 2013.
- [21] Z. Zhang, L. Juying, and Z. Mamat, “Sources identification and pollution evaluation of heavy metals in the surface sediments of Bortala River, Northwest China,” *Ecotoxicol. Environ. Saf.*, vol. 126, pp. 94–101, Apr. 2016, doi: 10.1016/j.ecoenv.2015.12.025.
- [22] A. El-Sikaily, A. Khaled, and A. El Nemr, “Heavy metals monitoring using bivalves from Mediterranean Sea and Red Sea,” *Environ. Monit. Assess.*, vol. 98, no. 1, pp. 41–58, 2004.
- [23] A. Khaled, A. El Nemr, and A. El Sikaily, “An assessment of heavy-metal contamination in surface sediments of the Suez Gulf using geoaccumulation indexes and statistical analysis,” *Chem. Ecol.*, vol. 22, no. 3, pp. 239–252, Jun. 2006, doi: 10.1080/02757540600658765.
- [24] N. F. Soliman, A. M. Younis, E. M. Elkady, and L. I. Mohamedein, “Geochemical associations, risk assessment, and source identification of selected metals in sediments from the Suez Gulf, Egypt,” *Hum. Ecol. Risk Assess.*, vol. 25, no. 3, pp. 738–754, 2019, doi: 10.1080/10807039.2018.1451301.
- [25] G. El Zokm, M. Shreadah, M. Masoud, and T. Said, “Assessment of heavy metals contamination in surface sediments of the Egyptian Red Sea coasts,” *Aust. J. Basic Appl. Sci.*, vol. 6, no. 6, pp. 44–58, 2012.
- [26] A. EL Nemr, A. Khaled, and A. EL Sikaily, “DISTRIBUTION AND STATISTICAL ANALYSIS OF LEACHABLE AND TOTAL HEAVY METALS IN THE SEDIMENTS OF THE SUEZ GULF,” *Environ. Monit. Assess.*, vol. 118, no. 1–3, pp. 89–112, Jul. 2006, doi: 10.1007/s10661-006-0985-9.
- [27] D. H. Youssef and G. F. El-Said, “A comparative study between the levels of some heavy metals in the sediments of two Egyptian contaminated environments,” *Chem. Ecol.*, vol. 26, no. 3, pp. 183–195, 2010, doi: 10.1080/02757541003785791.
- [28] X. Wang *et al.*, “Heavy metal contamination in surface sediments: A comprehensive, large-scale evaluation for the Bohai Sea, China,” *Environ. Pollut.*, vol. 260, p. 113986, 2020.
- [29] S. Caeiro, M. Costa, T. Ramos, ... F. F.-E., and U. 2005, “Assessing heavy metal contamination in Sado Estuary sediment: an index analysis approach,” *Elsevier*, 2005, Accessed: Jan. 27, 2021. [Online]. Available: <https://www.sciencedirect.com/science/article/pii/S1470160X05000051>.
- [30] H. E. Nour and A. S. El-Sorogy, “Heavy metals contamination in seawater, sediments and seashells of the Gulf of Suez, Egypt,” *Environ. Earth Sci.*, vol. 79, pp. 1–12, 2020.
- [31] J. Lario *et al.*, “Evolution of the pollution in the Piedras River Natural Site (Gulf of Cadiz, southern Spain) during the Holocene,” *Environ. Earth Sci.*, vol. 75, no. 6, p. 481, 2016.
- [32] A. El Nemr, G. F. El-Said, A. Khaled, and S. Ragab, “Distribution and ecological risk assessment of some heavy metals in coastal surface sediments along the Red Sea, Egypt,” *Int. J. Sediment Res.*, vol. 31, no. 2, pp. 164–172, 2016, doi: 10.1016/j.ijsrc.2014.10.001.
- [33] W. M. Badawy, A. El-Taher, M. V. Frontasyeva, H. A. Madkour, and A. E. M. Khater, “Assessment of anthropogenic and geogenic impacts on marine sediments along the coastal areas of Egyptian Red Sea,” *Appl. Radiat. Isot.*, vol. 140, pp. 314–326, 2018, doi: 10.1016/j.apradiso.2018.07.034.
- [34] M. E. Goher, H. I. Farhat, M. H. Abdo, and S. G. Salem, “Metal pollution assessment in the surface sediment of Lake Nasser, Egypt,” *Egypt. J. Aquat. Res.*, vol. 40, no. 3, pp. 213–224, 2014.

- [35] M. M. Dorgham, M. M. EL-Sherbiny, and M. H. Hanafi, "Environmental properties of the southern Gulf of Aqaba, Red Sea, Egypt," *Mediterr. Mar. Sci. Vol 13, No 2*, 2012, doi: 10.12681/mms.297.
- [36] M. Hamed, Y. Soliman, A. Soliman, A. Khodir, and F. Hussein, "Physico-chemical characteristics of Suez Bay water during 2006-2007," *Egypt. J. Aquat. Biol. Fish.*, vol. 14, no. 1, pp. 43–57, 2010.
- [37] A. H. Meshal, "A physical study of water pollution in Suez Bay (Hydrography of Suez Bay)." M. Sc. Thesis, Cairo University, Egypt, 1967.
- [38] R. L. Folk, *Petrology of sedimentary rocks*. Hemphill publishing company, 1980.
- [39] R. L. Folk, "Petrology of sedimentary rocks: Hemphill Pub," *Co., Austin, Texas*, vol. 63, 1974.
- [40] R. E. Carver, *Procedures in sedimentary petrology*. John Wiley & Sons Incorporated, 1971.
- [41] R. Passega, "Texture as characteristic of clastic deposition," *Am. Assoc. Pet. Geol. Bull.*, vol. 41, no. 9, pp. 1952–1984, 1957.
- [42] R. Passega, "Grain size representation by CM patterns as a geologic tool," *J. Sediment. Res.*, vol. 34, no. 4, pp. 830–847, 1964.
- [43] R. Passega and R. Byramjee, "Grain- size image of clastic deposits," *Sedimentology*, vol. 13, no. 3- 4, pp. 233–252, 1969.
- [44] G. S. Visher, "Grain size distributions and depositional processes," *J. Sediment. Res.*, vol. 39, no. 3, 1969.
- [45] E. Mycielska-Dowgiało and M. Ludwikowska-Kędzia, "Alternative interpretations of grain-size data from Quaternary deposits," 2011.
- [46] H. B. Stewart Jr, "Sedimentary reflections of depositional environment in San Miguel lagoon, Baja California, Mexico," *Am. Assoc. Pet. Geol. Bull.*, vol. 42, no. 11, pp. 2567–2618, 1958.
- [47] B. K. Sahu, "Multigroup discrimination of depositional environments using size distribution statistics," 1983.
- [48] L. Håkanson and M. Jansson, *Principles of Lake Sedimentology*. 1983.
- [49] H. L. Golterman, P. G. Sly, and R. L. Thomas, *Study of the relationship between water quality and sediment transport*. 1983.
- [50] D. E. Kimbrough and J. R. Wakakuwa, "Acid digestion for sediments, sludges, soils, and solid wastes. A proposed alternative to EPA SW 846 Method 3050," *Environ. Sci. Technol.*, vol. 23, no. 7, pp. 898–900, 1989.
- [51] K. Edgell, "USEPA method study 37: SW-846 Method 3050, acid digestion of sediments, sludges and soils. EPA Contract 68-03-3254," *Environ. Monit. Syst. Lab., Cincinnati, OH*, 1988.
- [52] D. E. Kimbrough and J. Wakakuwa, "Report of an Interlaboratory Study Comparing EPA SW 846 Method 3050 [1] and an Alternative Method from the California Department of Health Services," in *Waste Testing and Quality Assurance: Third Volume*, ASTM International, 1991.
- [53] A. Alharbi and A. El-Taher, "Elemental analysis of basalt by instrumental neutron activation analysis and inductively coupled plasma mass spectrometer," *J. Environ. Sci. Technol.*, vol. 9, no. 4, pp. 335–339, 2016, doi: 10.3923/jest.2016.335.339.
- [54] A. El-Taher and A. E. M. Khater, "Elemental characterization of Hazm El-Jalamid phosphorite by instrumental neutron activation analysis," *Appl. Radiat. Isot.*, vol. 114, pp. 121–127, 2016, doi: 10.1016/j.apradiso.2016.05.012.
- [55] D. E. Kimbrough and J. Wakakuwa, "A study of the linear ranges of several acid digestion procedures," *Environ. Sci. Technol.*, vol. 26, no. 1, pp. 173–178, 1992.
- [56] W. G. Rohrbough, "Reagent Chemicals, American Society Specifications, 7th ed." American Chemical Society: Washington, DC, 1986.
- [57] ISQG, "Interim sediment quality guidelines. Environment Canada, Ottawa, p 9,," Ottawa, 1995.
- [58] CCME, "Canadian Environmental Quality Guidelines Canadian Council of Ministers of the Environment, 2002, updated 2007, revised 2009," *Can. Environ. Qual. Guidel.*, no. Ccme 1991, pp. 1–8, 2009, Accessed: Jan. 28, 2021. [Online]. Available: https://www.elaw.org/system/files/sediment_summary_table.pdf.
- [59] E. R. Long, D. D. Macdonald, S. L. Smith, and F. D. Calder, "Incidence of adverse biological effects within ranges of chemical concentrations in marine and estuarine sediments," *Environ. Manage.*, vol. 19, no. 1, pp. 81–97, 1995, doi: 10.1007/BF02472006.
- [60] K. K. Turekian and K. H. Wedepohl, "Distribution of the elements in some major units of the earth's crust," *Geol. Soc. Am. Bull.*, vol. 72, no. 2, pp. 175–192, 1961.
- [61] S. R. Taylor, "Abundance of chemical elements in the continental crust: a new table," Pwgsmon Press Ltd, 1964. Accessed: Jan. 28, 2021. [Online]. Available: <https://www.sciencedirect.com/science/article/pii/0016703764901292>.
- [62] J. Usero, E. González-Regalado, and I. Gracia, "Trace metals in the bivalve molluscs *Ruditapes decussatus* and *Ruditapes philippinarum* from the Atlantic Coast of Southern Spain," *Environ. Int.*, vol. 23, no. 3, pp. 291–298, 1997, doi: 10.1016/S0160-4120(97)00030-5.
- [63] G. Müller, "Index of geoaccumulation in sediments of the Rhine River," *Geol. J.*, vol. 2, pp. 108–118, 1969, Accessed: Jan. 27, 2021. [Online]. Available: <https://ci.nii.ac.jp/naid/10030367619/>.
- [64] G. Müller, "Heavy metals in the sediment of the Rhine-Changes Seity," *Umsch. Wiss. Tech.*, vol. 79, pp. 778–783, 1979.
- [65] L. Boszke, T. Sobczyński, G. Głosińska, A. Kowalski, and J. Siepak, "Distribution of Mercury and Other Heavy Metals in Bottom Sediments of the Middle Odra River (Germany/Poland)," 2004. Accessed: Jan. 27, 2021. [Online]. Available: <http://www.pjoes.com/pdf-87689-21548?filename=21548.pdf>.
- [66] K. C. Schiff and S. B. Weisberg, "Iron as a reference element for determining trace metal enrichment in Southern California coastal shelf sediments," *Mar. Environ. Res.*, vol. 48, no. 2, pp. 161–176, 1999.
- [67] J. A. Baptista Neto, B. J. Smith, and J. J. McAllister, "Heavy metal concentrations in surface sediments in a nearshore environment, Jurujuba Sound, Southeast Brazil," *Environ. Pollut.*, vol. 109, no. 1, pp. 1–9, 2000, doi: 10.1016/S0269-7491(99)00233-X.
- [68] A. P. Mucha, M. T. S. D. Vasconcelos, and A. A. Bordalo, "Macrobenthic community in the Douro estuary: relations with trace metals and natural sediment characteristics," *Environ. Pollut.*, vol. 121, no. 2, pp. 169–180, 2003.
- [69] R. A. Sutherland, "Bed sediment-associated trace metals in an urban stream, Oahu, Hawaii," *Environ. Geol.*, vol. 39, no. 6, pp. 611–627, Apr. 2000, doi: 10.1007/s002540050473.
- [70] S. A. Sinex and G. R. Helz, "Regional geochemistry of trace elements in Chesapeake Bay sediments," *Environ. Geol.*, vol. 3, no. 6, pp. 315–323, Nov. 1981, doi: 10.1007/BF02473521.
- [71] L. Hakanson, "An ecological risk index for aquatic pollution control.a sedimentological approach," *Water Res.*, vol. 14, no. 8, pp. 975–1001, 1980, doi: 10.1016/0043-1354(80)90143-8.
- [72] D. L. Tomlinson, J. G. Wilson, C. R. Harris, and D. W. Jeffrey, "Problems in the assessment of heavy-metal levels in estuaries and the formation of a pollution index," vol. 33, no. 1–4, pp. 566–575, 1980, doi: 10.1007/BF02414780.
- [73] Y. Wang *et al.*, "Assessment of heavy metals in sediments from a typical catchment of the Yangtze River, China," *Env. Monit Assess.*, vol. 172, no. 1–4, pp. 407–417, Jan. 2011, doi: 10.1007/s10661-010-1343-5.
- [74] B. Wei *et al.*, "Heavy metal induced ecological risk in the city of Urumqi, NW China," *Env. Monit Assess.*, vol. 160, no. 1–4, pp. 33–45, Jan. 2010, doi: 10.1007/s10661-008-0655-1.
- [75] M. Ludwikowska-Kędzia, "Evolution of the middle segment of the Belnianska River valley in the Late Glacial and Holocene."

- Dialog Press, Warsaw, 2000.
- [76] J. Szmańda, "Grain-transport conditions: an interpretative comparison on the analysis of C/M diagrams and cumulative curve diagrams, with the overbank deposits of the Vistula River, Toruń, as an example," *Rekonstrukcja Dynamiki Procesów Geomorfol. Rzeźby i osad y. Smolska, E., Giriat, D., eds., Uniw. Warsz. Wyzd. Geogr. i Stud. Reg. Kom. Badań Czwartorzędu*, pp. 367–376, 2007.
- [77] W. G. H. Maxwell, "Atlas of the great barrier reef," 1968.
- [78] J. Castro, *Effects of sediment on the aquatic environment: potential NRCS actions to improve aquatic habitat*, no. 6. US Department of Agriculture, Soil Conservation Service, 1995.
- [79] A. M. Mansour, M. S. Askalany, H. A. Madkour, and B. B. Assran, "Assessment and comparison of heavy-metal concentrations in marine sediments in view of tourism activities in Hurghada area, northern Red Sea, Egypt," *Egypt. J. Aquat. Res.*, vol. 39, no. 2, pp. 91–103, 2013, doi: 10.1016/j.ejar.2013.07.004.
- [80] I. H. Lotfy, A. I. L. Beltagy, Y. A. Ali, A. I. L. Beltagy, and M. Lotfy, "Grain size analysis, areal distribution of sediments and environment of deposition of tidal and bottom sediments from Ghardaqa region, Red Sea area," *Bull. Inst. Ocean. Fish.*, vol. 13, pp. 147–167, 1987.
- [81] H. I. Farhat, "Textural features and transportation mode of Nile Delta coastal lagoon surficial sediments (Lake Burullus, Ramsar Site)," *SN Appl. Sci.*, vol. 1, no. 9, pp. 1–12, 2019.
- [82] P. Parthasarathy *et al.*, "Sediments Dynamics and Depositional Environment of Coleroon River Sediments, Tamil Nadu, Southeast Coast of India," *J. Coast. Sci. 3 1-7pp*, 2016.
- [83] D. B. Duane, "Significance of skewness in recent sediments, western Pamlico Sound, North Carolina," *J. Sediment. Res.*, vol. 34, no. 4, pp. 864–874, 1964.
- [84] R. L. Folk, "A review of grain- size parameters," *Sedimentology*, vol. 6, no. 2, pp. 73–93, 1966.
- [85] D. H. Youssef, · Ghada, F. El-Said, D. H. Youssef, and G. F. El-Said, "Assessment of some heavy metals in surface sediments of the Aqaba Gulf, Egypt," *Env. Monit Assess.*, vol. 180, no. 1–4, pp. 229–242, Sep. 2011, doi: 10.1007/s10661-010-1784-x.
- [86] D. M. S. A. Salem, A. Khaled, A. El Nemr, and A. El-Sikaily, "Comprehensive risk assessment of heavy metals in surface sediments along the Egyptian Red Sea coast," *Egypt. J. Aquat. Res.*, vol. 40, no. 4, pp. 349–362, 2014, doi: 10.1016/j.ejar.2014.11.004.
- [87] M. M. Storelli, A. Storelli, and G. O. Marcotrigiano, "Heavy metals in the aquatic environment of the Southern Adriatic Sea, Italy: Macroalgae, sediments and benthic species," *Environ. Int.*, vol. 26, no. 7–8, pp. 505–509, 2001, doi: 10.1016/S0160-4120(01)00034-4.
- [88] S. Topcuoğlu, Ç. Kirbaşoğlu, and N. Güngör, "Heavy metals in organisms and sediments from Turkish coast of the Black Sea, 1997-1998," *Environ. Int.*, vol. 27, no. 7, pp. 521–526, 2002, doi: 10.1016/S0160-4120(01)00099-X.
- [89] F. Li *et al.*, "Spatial risk assessment and sources identification of heavy metals in surface sediments from the Dongting Lake, Middle China," *J. Geochemical Explor.*, vol. 132, pp. 75–83, Sep. 2013, doi: 10.1016/j.gexplo.2013.05.007.
- [90] A. Y. Kahal, A. S. El-Sorogy, H. J. Alfaiḫ, S. Almadani, and H. A. Ghrefat, "Spatial distribution and ecological risk assessment of the coastal surface sediments from the Red Sea, northwest Saudi Arabia," *Elsevier*, 2018, doi: 10.1016/j.marpolbul.2018.09.053.
- [91] P. S. Harikumar, ; U P Nasir, and ; M P Mujeebu Rahman, "Distribution of heavy metals in the core sediments of a tropical wetland system," *Int. J. Environ. Sci. Tech.*, vol. 6, no. 2, pp. 225–232, 2009.